Textures and Microstructures, 1991, Vols 14–18, pp. 775–780
Reprints available from the publisher
Photocopying permitted by license only

MODEL OF SECONDARY RECRYSTALLIZATION IN SILICON-IRON AND COMPARISON WITH EXPERIMENTS

G. ABBRUZZESE, A. CAMPOPIANO, S. FORTUNATI

Centro Sviluppo Materiali - C.P. 10747 Roma-Eur, Italy

ABSTRACT

A comparative analysis has been made of selective grain growth processes at different layers of a grain oriented silicon iron sheet. Shorter incubation time and best orientation selection during secondary recrystallization appear at 40 μm from the sheet surface. This has been linked to the presence of a relatively strong <001>//RD fiber in the texture. The differences through the sheet thickness are assumed to be inherited from the hot band. Computer simulations in the framework of the statistical theory of grain growth support the proposed selection mechanisms.

INTRODUCTION

It is well known that in industrial Fe3%Si sheet, Goss texture develops by secondary recrystallization that occurs in the presence of grain growth inhibitors (second phase particles or foreign atoms in solid solution) [1,2]. Secondary recrystallization is characterized by a selective process due to a special orientation relationship between Goss and matrix grains [3,4]. The aim of the work reported here was to obtain more detailed information about the orientation selection process through the sheet thickness [5], collecting experimental data on the evolution of grain size distribution of various texture components during the grain growth process and interpreting the process by computer simulation based on a statistical model of grain growth [2,3,4,6,7].

EXPERIMENTAL

An investigation was made of grain growth in a 3%Si-Iron from primary recrystallized sheet obtained from an industrial heat (C=0.035%, Mn=0.07%, S=0.025%, Cu=0.15%) that provided good final magnetic properties (B_{800}=1.85 T, $P_{1.7}$=1.06 W/kg).
A sheet sample (300x30x0.22 mm) was heat treated in a temperature gradient furnace [2,3] up to 930°C (1 h soaking time) with a heating rate of 30°C/h. The tie-in between temperature and the position along the sample length allows the abnormal grain growth starting temperature to be singled out by simple grain size inspection. Three soaking temperatures, namely 830°C, 850°C and 890°C (the last one just before secondary recrystallization) have been choosen.
An etch-pitting technique and QTM analysis [5,8] were used to evaluate the grain size distributions of the {111}<112>, {111}<110>, {110}<001>, {100}<011> and {100}<001> orientation classes.

The measurements were performed on layers parallel to the rolling plane at 40,70 and 100 μm from the sheet surface (about 1/5, 1/3, 1/2 of the sheet thickness, respectively). The sample treated at the intermediate temperature (850°C) has not been measured at the 70 μm layer.
Statistical samples of about 2000 grains were measured for each observed layer. The orientation classes are defined as follows: the {111}<112> and {111}<110> classes contain grains having an angular dispersion cone of $\pm$15° around <111>//normal direction (ND), the {100}<001> class of $\pm$30° around <001>//rolling direction (RD), the {100}<011> class of $\pm$15° around <011>// RD and the {110}<001> class of $\pm$15° around both ND and RD.
Moreover the {110}<001> orientation class, analysed at 40 and 70 μm was divided into a {110}<001> class within $\pm$5° and a {110}<001> class dispersed from $\pm$ 5° to $\pm$ 15°.
X-ray analysis and Orientation Distribution Function (ODF) calculations were performed on all the analysed layers.

EXPERIMENTAL RESULTS

Statistical parameters of the measurements are summarized in Table 1.

DIST. FROM THE SURFACE (μm)	MEAN RADIUS (μm)									VARIANCES (μm^2)								
	40			70		100				40			70		100			
TEMP. (°C)	830	850	890	830	890	830	850	890		830	850	890	830	890	830	850	590	
{111}<112>	6.1	7.3	8.2	7.5	8.1	6.3	6.7	7.4		3.0	4.6	5.8	3.6	4.5	4.5	4.1	5.1	
{111}<110>	6.4	7.3	7.9	7.7	8.8	7.1	6.9	7.7		3.2	3.9	6.3	5.0	5.3	4.1	4.0	3.8	
{110}<001> (5°-15°)	6.5	7.3	8.5	8.7	9.5					3.0	5.0	8.0	5.9	5.4				
						6.9	7.5	8.4							4.6	6.0	7.6	
{110}<001> (0°-5°)	6.5	7.2	8.5	7.5	8.9					4.0	7.0	16.0	6.4	9.8				
{100}<001>	6.4	7.1	8.6	7.3	8.6	6.5	7.5	7.6		3.0	6.5	8.1	4.4	6.9	3.6	3.3	5.6	
{100}<011>	6.5	6.9	7.5	7.2	8.3	6.6	7.0	7.6		2.8	4.1	5.3	4.6	5.2	5.1	5.3	4.2	
Average	6.4	7.2	8.1	7.6	8.6	6.7	7.1	7.8		3.0	4.6	7.1	4.6	5.7	4.4	4.6	5.4	

DIST. FROM THE SURFACE (μm)	VOLUME FRACTIONS (%)								
	40			70		100			
TEMP. (°C)	830	850	890	830	890	830	850	890	
{111}<112>	11.0	22.8	22.3	18.8	16.7	13.2	14.3	13.0	
{111}<110>	17.7	23.1	15.8	23.8	19.6	23.3	19.7	17.9	
{110}<001> (5°-15°)	5.0	8.5	11.7	8.1	11.3				
						16.0	16.4	20.0	
{110}<001> (0°-5°)	3.7	5.7	9.5	5.9	7.4				
{100}<001>	38.0	10.8	10.0	12.0	14.5	8.9	11.7	10.6	
{100}<011>	15.0	11.2	8.0	9.4	9.3	13.9	14.6	12.8	

Table 1 - Experimental values of mean radius, distribution variances and volume fractions. The table is lacking of the "background" component, that includes all the grains not belonging to the six classes considered.

During sheet annealing, Goss grains and nearby orientation grow faster at 40 μm from the surface than in the other layers, in fact the variance of the more precise Goss grains distribution is found to increase markedly at this layer. This is the result of an higher driving force to growth produced by the combination of a smaller average grain size and a relatively high heterogeneity of the matrix (variance) [9].
The foregoing confirms the Goss grain abnormal growth starts at about 1/5 of the sheet thickness [2].
At 70 μm there is quite continuous grain growth with all texture components growing in a similar manner. Furthermore, the grain size increase from 830°C up to near secondary recrystallization temperature (890°C) is quite small compared to that measured at 40 μm, probably due to the slightly bigger mean size of the grains.
In any case, it ensues that Goss grains always grow faster than the other texture components even when they have no initial size advantage in the system [2-5].
Another marked peculiarity of the 40 μm layer is the orientation distribution corresponding to the first stage of grain growth (830°C). The <001>// RD fiber has the larger volume fraction while at 100 and 70 μm from the surface the "cube on corner" or γ-fiber (<111>//ND) constitutes the major volume fraction followed by the "cube on face" (<100>//ND) component.
These differences could be responsible for the shorter incubation time of Goss abnormal grain growth at 1/6-1/4 depth of the sheet thickness in these materials [2,4,5].

COMPUTER SIMULATIONS AND DISCUSSION

The origin of the particular texture present at 40 μm from the surface is the heritage of elongated Goss grains within an angular dispersion of 15° that are formed and typically observed at 1/6-1/4 thickness of the hot band [10]. X-ray analysis through hot band thickness typically reveals strong intensity of the {110}<001> orientation concentrated at that particular layer [10]. The elongated grains are generated by a deformation and recovery process of Goss nuclei that are in easy glide condition (stable end orientation) under the particular stress field present at that sheet layer during hot-rolling (shear stresses). During cold rolling these big grains behave partially like monocrystals with orientation dispersed around {110}<001> which rotate around <110> up to {111}<112> the yield increasing with the rolling degree. After recrystallization there is a marked intensity of Goss nuclei together with {310}<001> and {210}<001> grains as minor components, or vice-versa, depending on the cold reduction level applied [11]. This alternate majority-minority role played by the orientation belonging to the <001>//RD fiber after recrystallization reveals the presence of a special relationship in terms of boundary mobility existing between one and the other. This kind of relationship has been observed elsewhere (15-30° around <001>) during selective secondary recrystallization processes [12,13].
Observation at the orientation distribution evolution at the 40 μm layer during grain growth (Table 1) reveals the orientation relationship contributions to the Goss grain selection mechanism. In fact, at the first stages of grain growth (830°C) a relatively strong <100>//RD is present while the γ-fiber (especially near {111}<112>) is depressed. Of course, in order to ensure a good selective growth [14] Goss grain must be a minority component in the whole texture and must have a special boundary relationship with the main texture component. In B.C.C. system bulk this is found at 27° around <011>, corresponding to a strong {111}<112>, {554}<225> texture. Thus at 40 μm there is an initial apparentely unfavourable situation. However, during grain growth the {111}<112> volume fraction increases strongly (Table 1) becoming the main component after an hour's treatment at 850°C. This selective growth corresponds to a depression of the <001>//RD fiber

(Fig. 1), mainly classified by the etch pitting technique in the {100}<001> and the dispersed {110}<001> orientation classes.
This indicates that the more dispersed {110}<001> class behaves as a booster (in terms of boundary relationship) for the growth of the γ-fiber components. The proper Goss orientation class ({110}<001>, 0-5° of dispersion cone) performs initial selective growth mainly by taking advantage of the strong presence of <001>//RD fiber components at 15-30 degrees around <001> (Fig. 1) that produce favourable surroundings for Goss grains consisting of boundaries with higher mobility and lower energy [3,15] than those experienced by the matrix grains. The faster selective growth at the 40 μm layer is thus induced by the alternating favourable orientation relationship that Goss grains have in the polycrystalline system during texture evolution. Moreover the final magnetic properties of grain oriented silicon iron depend directly on the amount of crystals having <001> direction parallel to that of rolling irrespective of the crystal plane lying on the sheet surface. In fact the studied material, as fully secondary recrystallized, also exhibits the presence of a certain amount of {210}<001>, {310}<001> oriented grains. Moreover the same measurements performed on the sample position where secondary recrystallization is just developing, revealed a larger amount of grains of the relevant orientations, showing that these texture components also participate in the selection process though more slowly than Goss grains.
The selection of Goss grains through the <100>//RD fiber, which conserves this favourable magnetic character, should thus be more effective in developing good magnetic permeability than that obtained by consumption of the more dispersed {111}<112> and nearby texture components.
To confirm the validity of the discussed mechanism, computer simulations were performed using the grain growth statistical model [6,14] and assuming boundary energy and mobility values, between the various orientation classes considered, in qualitative agreement with the conclusions of the preceding discussion. For the first time [2-5] the contemporaneous behaviour of four different texture components was simulated in order to reproduce the complex texture evolution obtained from the experimental data at 40 μm from the sheet surface. Experimental and calculated grain size distributions (the last ones obtained with an Inhibition value of I_Z=12 m^{-1} [6]) for this layer are shown in Fig. 2, while in Table 3 a number of their detailed statistical parameters are compared at the same total mean radius. There is substantial agreement between the two groups of data resulting from the realistic boundary conditions indicated in Table 2. The main differences between experimental and simulated results concern the Goss orientation (dispersion around <100> less than 5°).

Tab. 2 - Boundary parameter values used in computer simulations. The four texture components studied are represented by
T = {111}<112> and {111}<110> grains with a 15° conic dispersion around ND.
G = {110}<001> grains $\pm$5° around RD.
GD= Grains from $\pm$5° up to $\pm$15° around both <001>//RD and <110>//ND.
M = All the remaining texture components.

BOUNDARY	M-M	T-M	GD-M	G-M	GD-T	G-T	G-G	GD-GD	G-GD	T-T
ENERGY ($J\ m^{-2}$)	0.65	0.38	0.35	0.30	0.36	0.33	0.25	0.25	0.26	0.45
MOBILITY ($10^{-12}\ m^4\ J^{-1}\ K^{-1}\ s^{-1}$)	0.4	2.5	2.5	2.5	2.3	2.5	0.1	0.1	0.1	0.2

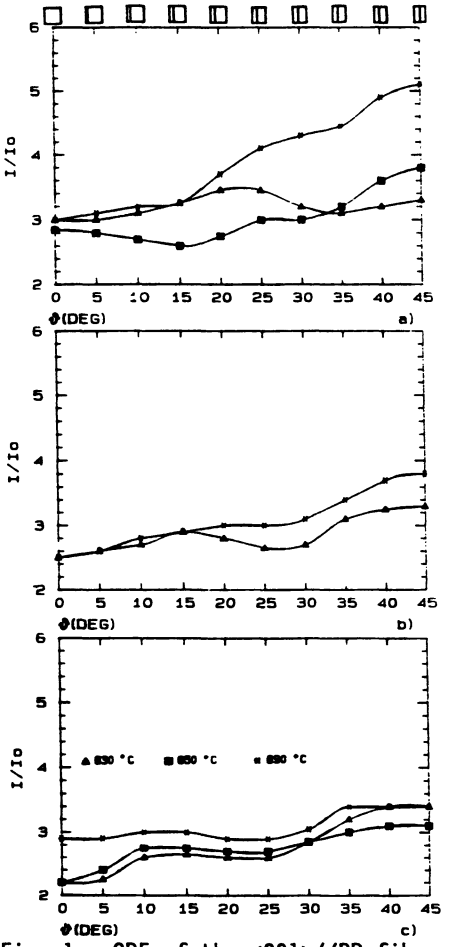

Fig. 1 - ODF of the <001>//RD fiber in the different specimens analysed at a) 40 μm, b) 70 μm and c) 100 μm from the sheet surface at three annealing temperatures.

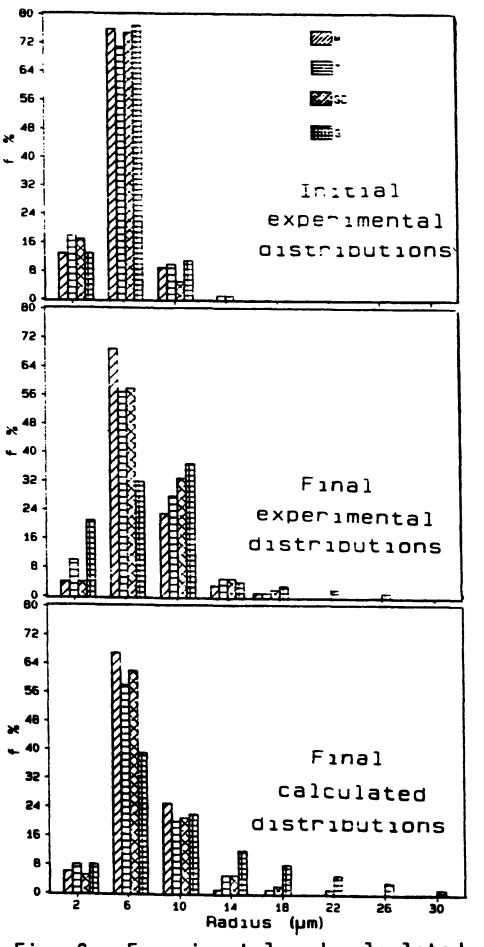

Fig. 2 - Experimental and calculated grain size distributions of four texture components at 40 μm from the sheet surface. Every distribution is normalized to 100.
T = {111}<112> and {111}<110> grains with a 15° conic dispersion around ND
G = {110}<001> grains ±5° around RD
GD= Grains from ±5° up to ±15° around both <001>//RD and <110>//ND
M = All the remaining texture components.

The cause of these can be explained by the following: a) the experimental statistic for the minority orientation classes is rather poor (about 100 grains for Goss orientation) compared with the whole set of grains (~2000). This is a serious limitation when comparisons of size distribution shapes are involved, as these are very sensitive to the size of the statistical set (especially for the distribution tails); b) the description of the texture by four orientation classes is a further step towards full representation of the measured texture, but it still remains an approximation of the complex interactions between the many orientations present in the real microstructure. On the other hand the main obstacle to achieving a full description of texture evolution is the lack of a reliable model capable of

evaluating mobility and energy of any boundary.

Table 3 - Values of mean radius, volume fractions and distribution variances coming from experimental and simulated grain growth at 40 μm from the surface. Texture components considered are the same as in Table 2.

	MEAN RADIUS (μm)				VOLUME FRACTIONS (%)				VARIANCES (μm^2)			
	EXPERIMENTAL			CALCULATED					EXPERIMENTAL			CALCULATED
T (°C)	830	850	890	830 850 890	830	850	890	830 850 890	830	850	890	830 850 590
M	6.2	7.0	8.0	6.2 7.1 7.6	66.0	39.0	37.0	66.0 42.0 32.0	3.0	4.5	5.0	3.0 3.3 4.0
T	6.1	7.3	8.0	6.1 7.0 8.0	25.0	46.0	40.0	25.0 34.0 32.0	3.0	4.3	6.0	3.0 5.0 8.0
G	6.5	7.2	8.5	6.5 9.4 10.8	4.0	6.0	12.0	4.0 16.0 26.0	4.0	7.0	16.0	4.0 9.0 36.0
GD	6.5	7.3	8.5	6.5 7.2 8.0	5.0	9:0	11.0	5.0 8.0 10.0	3.0	5.0	8.0	3.0 4.5 10.0
Average	6.2	7.2	8.1	6.2 7.2 8.1					3.0	4.6	7.1	3.0 4.4 8.3

CONCLUSIONS

The comparative analysis of grain size distributions through the thickness of a heat-treated silicon iron sheets shows that there are significant differences in Goss grains selection at different depths from the surface. In particular at about 1/5 of the sheet thickness the selection of Goss grains appears more effective than in the bulk of the material. This peculiar behaviour has been connected with the favourable presence of a stronger <100>//RD fiber in the layer closer to the sheet surface which is assumed to be inherited by the texture and microstructure heterogeneities already present at the hot band level. This mechanism has been confirmed by comparing the experimental results with the predictions of the statistical model of grain growth.

REFERENCES

1. T. Gladman, Proc. Roy. Soc. London 294A, 298 (1966).
2. G. Abbruzzese, S. Fortunati, J. Appl. Phys. 64, 10 (1988).
3. G. Abbruzzese, S. Fortunati, Physica Scripta, 39, 624 (1989).
4. G. Abbruzzese, I. Ciancaglioni, A. Campopiano, Texture and Microstructure 8, 401 (1988).
5. G. Abbruzzese, S. Fortunati, A. Campopiano, Proc. of SMM9, El Escorial (1989).
6. G. Abbruzzese, Acta Met., 33, 1329 (1985).
7. G. Abbruzzese, A. Campopiano, Proc. of Recrystall. 90, Sydney (1990).
8. S. Fortunati, G. Abbruzzese, to be presented at the Int. Conf. on "Grain Growth in Polycrystalline Materials" , 18-21 June 1991, Rome.
9. G. Abbruzzese, IEEE Transaction on Magnetics, 25, 3955 (1989).
10. Mishra, C. Darmann, K. Lücke, Acta Met., 32, 2185 (1984).
11. T. Taoka, E. Furubajashi, S. Takeuchi, ISIJ, 7, 95 (1967).
12. T. Fujii, Y. Hiraoka, M. Okada, R. Watanabe, Proc. of the 7° ICOTOM Conference, Holland (1984).
13. T. Fujii, Y. Hiraoka, M. Okada, R. Watanabe, J. Less Comm. Met., 99, 77 (1984).
14. G. Abbruzzese, K. Lücke, H. Eichelkraut, Proc. of the 8° ICOTOM Conference, Santa Fe, New Mexico (1987).
15. R. Shimizu, J. Harase, Acta Met. 37, 1241 (1989).